

Position and Force Control Based on Mathematical Models of Pneumatic Artificial Muscles Reinforced by Straight Glass Fibers

Taro Nakamura and Hitomi Shinohara

Chuo University

Faculty of Science and Engineering, Department of Precision Mechanics
1-13-27 Kasuga, Bunkyo-ku, Tokyo 112-8551 Japan

nakamura@mech.chuo-u.ac.jp

Abstract - This paper reports on the position and force control of pneumatic artificial muscles reinforced by straight glass fibers. This type of artificial muscle has a greater contraction ratio and power and a longer lifetime than conventional McKibben types. However, these muscles are highly non-linear; hence, it is difficult to use them in a mechanical system. Furthermore, this actuator has a high compliance characteristic. Though this characteristic is useful for human interactions, the position and force of this actuator cannot be easily controlled.

In this paper, a mathematical model of this type of artificial muscle is proposed, and the relationship between design parameters and control specifications is realized. In addition, the position and force based on the mathematical model are determined and applied to artificial muscle linearization.

Index Terms – Pneumatic artificial muscle, mathematical model, feed-forward linearization, position control

I. INTRODUCTION

Pneumatic muscle actuators have lower weight, higher force and greater flexibility than other actuators. Therefore, they are in the spotlight as actuators for rehabilitation robots [1] and power assist robots [2] and to provide similar functions elsewhere.

Artificial muscles reinforced by straight glass fibers have been developed [3]. This type of muscle has a greater contraction ratio and power and a longer lifetime than conventional McKibben types [4]. In addition, in dynamic evaluations they have almost the same characteristics as human muscles in performing isotonic and isometric contractions [5][6][7]. However, since this type of muscle is highly non-linear, the position and force of this actuator cannot be easily controlled. Furthermore, because there are many parameters comprising an artificial muscle, experimental inspection is needed to create a geometrical shape satisfying control specifications.

In this paper, a mathematical model of the artificial muscle reinforced by straight fibers is proposed, and the relationship between design parameters and control specifications is realized. In addition, the position and force control

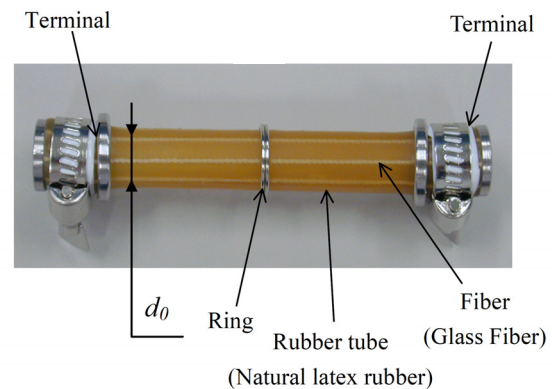


Fig. 1 A photograph of the artificial muscle.

based on the mathematical model are determined and applied to the artificial muscle.

This paper consists of six sections. In the second section, the artificial muscle reinforced by straight fibers used in this research is explained. In the third section, a geometric model is decided upon, and a mathematical model is derived from a state of mechanical equilibrium developed with air pressure. In the fourth and fifth sections, the position and force control based on the mathematical model is examined and applied. In the sixth section, the results from this research are summarized.

II. THE PNEUMATIC ARTIFICIAL MUSCLE REINFORCED BY STRAIGHT FIBERS

Fig.1 shows a photograph of the artificial muscle. The tube is made from natural latex rubber, with glass fibers inserted in the long axis direction and fixed at either end by a terminal. When a certain pressure is created in the tube, because the muscle can only expand in the radial direction, the contraction occurs in the axis direction. The rings installed on the tube are able to change the ratio between the length and diameter of the muscle.

III. DERIVATION OF THE MATHEMATICAL MODEL OF THE ARTIFICIAL MUSCLE

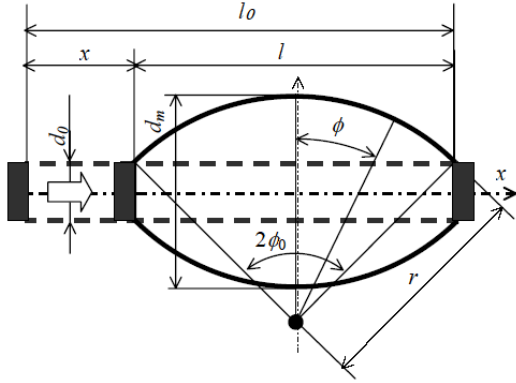


Fig. 2 The shape model of the artificial muscle from the Z-axis view.

A. A geometric model of the artificial muscle

Before developing the mathematical model, the shape coefficients were determined from the internal pressure occurring in the muscle. In this case, based on Pascal's principle, we assumed that the pressure occurs in a radial direction in the inner tube. Hence, when the artificial muscle is contracted, a cross section of the axial direction is assumed to have the circular shape shown in Fig. 2.

From Fig. 2, the following equations are derived:

$$r = \frac{l_0}{2\phi_0} \quad (1)$$

$$\frac{l_0 - l}{l_0} = \frac{x}{l_0} = 1 - \frac{\sin \phi_0}{\phi_0} \quad (2)$$

$$\frac{d_m - d_0}{l_0} = \frac{1 - \cos \phi_0}{\phi_0} \quad (3)$$

Here, the initial length and diameter are l_0 and d_0 , respectively. The length and the maximum diameter when the muscle is contracted are l and d_m , respectively. Finally, the shape of a circular curve is indicated by a radius r and central angle $2\phi_0$, respectively. The range of ϕ_0 is $0 < \phi_0 < \pi/2$; x is the contraction length expressed as $x = l_0 - l$.

Next, the geometric model given by the above expressions is compared with the geometric shape of the actual artificial muscle. Fig. 3 shows the relationship between the contraction and the maximum diameter when the ratio between the length and diameter is changed and the muscle takes on a load. The experimental curve is a dimensionless contraction and expansion with an initial length l_0 . The theoretical curve applies eq.(2) and (3). These figures show that the experimental curve is almost the same as the theoretical curve regardless of the change in the load and l_0/d_0 ratio. Therefore, there is no hindrance even if the geometric model of this artificial muscle is assumed to be a circle.

The circular shape of this artificial muscle is determined by two variables, r and ϕ_0 . If the feed-forward control is applied to the muscle in real time, it is also desirable to have only contractions that can be measured in real time by a sensor. Therefore, in this paper we try to estimate a curve model to determine function-only contractions.

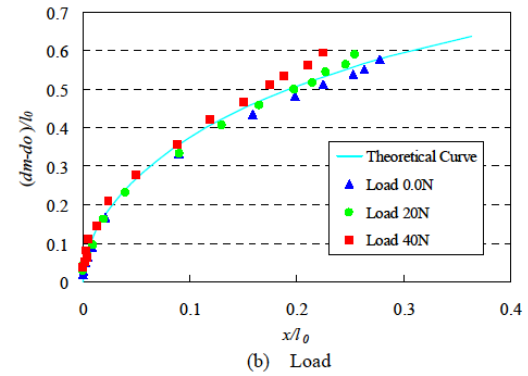
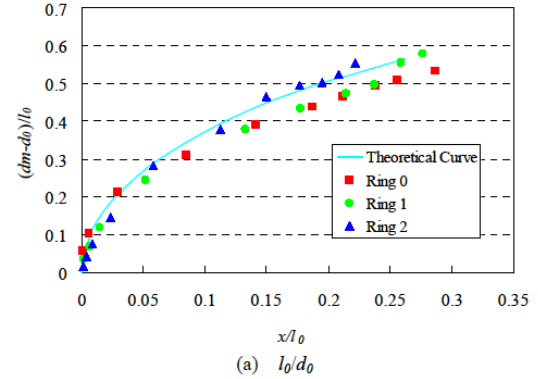


Fig. 3 Theoretical and experimental results of the relationship between contraction ratios and expansion ratio

Using eq.(2) and (3), the ϕ_0 is expressed by the following equation:

$$\phi_0 = \frac{2l_0(d_m - d_0)}{(l_0 - x)^2 + (d_m - d_0)^2} \quad (4)$$

An approximation of the theoretical curve is expressed by the following equation:

$$d_m = \alpha(xl_0)^{0.5} - d_0 \quad (0 \leq x \leq 0.363l_0) \quad (5)$$

As a result of an approximation by the least-square method, α is 0.75. Then, using eq. (1), (4), and (5), we express ϕ_0 as

$$\phi_0(x) = \frac{2\alpha l_0^{1.5} x^{0.5}}{(l_0 - x)^2 + \alpha^2 x} \quad (6)$$

B. The mechanical equilibrium model

A mechanical equilibrium model using the external load and air pressure is expressed based on the geometric model. The following conditions are assumed:

- When the artificial muscle expands, the thickness of rubber remains constant.
- Young's modulus of glass fibers has a much larger value than that of natural rubber; glass fibers do not stretch.
- The number of fibers is an even number.

Fig. 4 shows a 3-dimensional quarter model of the artificial muscle. It is best to assume mechanical equilibrium in both the axial direction (X axis direction) and radial direction (Y

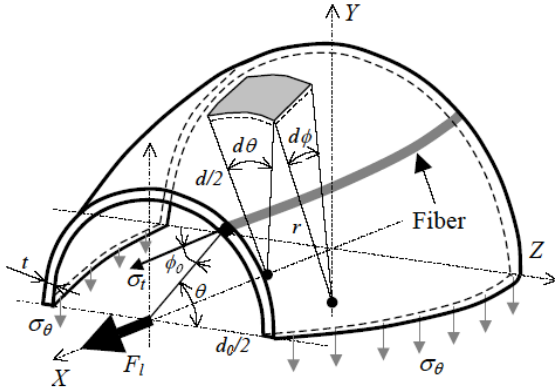


Fig. 4 A 3-D quarter model of the artificial muscle.

axis direction) in this artificial muscle.

(1) Mechanical balance in the axial direction

A mechanical equilibrium model of the axial direction was derived. P is the pressure impressed on the inside of the artificial muscle, and σ_t is the stress due to the tension of the fibers. The resultant forces in the x -axis direction P_x and S_x are expressed by the following equation:

$$P_x = \frac{\pi P d_0^2}{4} \quad (7)$$

$$S_x = -n b t_i \sigma_t \cos \phi_0 \quad (0 \leq n b \leq \pi d_0), \quad (8)$$

where n is the number of fibers, b is the width, and t_i is the thickness. If F_l is the load impressed on the artificial muscle, then the equilibrium in the x -direction is expressed by the following equation:

$$P_x + S_x + F_l = 0 \quad (9)$$

Therefore, σ_t is expressed by the following equation:

$$\sigma_t = \frac{4F_l + \pi P d_0^2}{4n b t_i \cos \phi_0} \quad (10)$$

(2) Mechanical balance in the X-Z plane

A mechanical equilibrium model in the X - Z plane was derived. The resultant force in the radial direction consists of the elasticity of the rubber S_θ , the force of the Y -direction ingredient that caused the tension in the fibers, and the resultant P_y of the Y -direction ingredient derived from the pressure P .

The elastic force of the rubber S_θ was examined. The distortion of radial-direction rubber is expressed by the following equation (Fig.2):

$$\frac{d - d_0}{d_0} = \frac{2r(\cos \phi - \cos \phi_0)}{d_0} \quad (11)$$

Taking σ_θ as the stress of the rubber, the following equation is derived:

$$\sigma_\theta = \frac{K}{d_0}(d - d_0) = \frac{2rK}{d_0}(\cos \phi - \cos \phi_0) \quad (12)$$

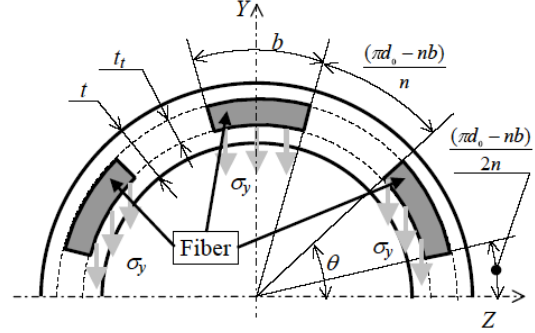


Fig. 5 The shape model of the artificial muscle from the X -axis view.

K is the elasticity coefficient of natural rubber used in the artificial muscle; it equals 22.4kPa. By integrating eq. (12) in the central angle ϕ_0 of a circular shape, the elasticity of rubber S_θ is expressed by the following equation:

$$S_\theta = 4t \int_0^{\phi_0} \sigma_\theta r d\phi = \frac{8r^2 K t}{d_0} (\sin \phi_0 - \phi_0 \cos \phi_0) \quad (13)$$

where t is the thickness of the artificial muscle.

The resultant force in the radial-direction axis

S_y , which causes the tension in the fibers, was examined.

Fig. 5 shows the shape model of the artificial muscle from the view of the X -axis. S_y is expressed by the following equation (Figs. 4 and 5):

$$S_y = M d_0 t_i \sigma_y = M d_0 t_i \sigma_t \sin \phi_0 \quad (0 \leq M \leq 2) \quad (14)$$

M is the coefficient for the fibers of the artificial muscle and is expressed by the following equation:

$$M = \sum_{m=1}^{\frac{n}{2}} \int_{L(m) - \frac{b}{2d_0}}^{L(m)} \sin \theta d\theta \quad (m=1,2,3,\dots) \quad (15)$$

$$L(m) = \frac{(2m-1)(\pi d_0 - nb)}{n d_0} + \frac{mb}{2d_0} \quad (16)$$

When eq. (10) is substituted for eq. (14), the following equation results:

$$S_y = \frac{d_0 M (4F_l + \pi P d_0^2)}{4n b} \tan \phi_0 \quad (17)$$

The resultant force in the radial-direction axis P_y is calculated by the following equation:

$$P_y = -4 \int_{\frac{d_0}{2}}^{\frac{d_m}{2}} dx \int_{-\frac{\pi}{2}}^{\frac{\pi}{2}} P \cos \theta \frac{d}{2} d\theta \quad (18)$$

Equations eq. (19) and eq. (20) are derived from Fig. 4.

$$\frac{d}{2} = \frac{d_0}{2} + r(\cos \phi - \cos \phi_0) \quad (19)$$

$$dx = -r \cos \phi d\phi \quad (20)$$

When eq. (18) is substituted by eq. (19) and (20) and integrated, P is expressed by the following equation:

$$P_y = -4rP(r\phi_0 - r \sin \phi_0 \cos \phi_0 + d_0 \sin \phi_0) \quad (21)$$

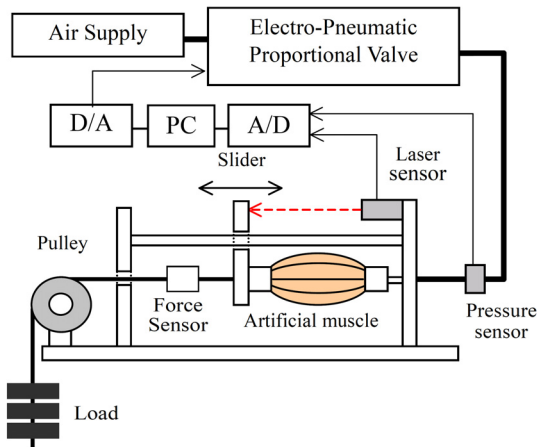


Fig. 6 Configuration of the experimental system.

The resultant force equilibrium in the X - Z plane is expressed by the following equation:

$$S_x + S_y + P_y = 0 \quad (22)$$

When eq. (22) is substituted by eq. (13), (14), and (21) and re-ordered, P is expressed by the following equation:

$$P = \frac{\frac{2Kt}{d_0} \left(\frac{l_0}{d_0} \right)^2 \left(\frac{\sin \phi_0 - \phi_0 \cos \phi_0}{\phi_0^2} \right) + \frac{F_r M}{d_0 n b} \tan \phi_0}{\left\{ \left(\frac{l_0}{d_0} \right)^2 \left(\frac{\phi_0 - \sin \phi_0 \cos \phi_0}{\phi_0^2} \right) + 2 \left(\frac{l_0}{d_0} \right) \frac{\sin \phi_0}{\phi_0} \right\} - \frac{\pi d_0 M}{4 n b} \tan \phi_0} \quad (23)$$

When eq. (23) is substituted by eq. (6), the expression of the relationship between the contraction x and pressure P is found. The first term of the numerator concerns the expansion of the rubber; the other term concerns the load. The first term of denominator concerns the internal expansion pressure; the other concerns the fibers of the artificial muscle.

IV. EXPERIMENTAL RESULTS AND DISCUSSION

The validity of the mathematical model was examined experimentally. Concretely, the experimental result of the relationship between the pressure and the contraction ratio with changes in the ratio of l_0/d_0 or the load was compared with the theoretical curve given by the mathematical model.

A. The experimental system and specifications of the artificial muscle

Fig. 6 shows the experimental system using the artificial muscle. Pressure is applied to the artificial muscle through

Table 1. Specifications of the artificial muscle.

Outer Diameter of the Tube	15.0 mm
Inner Diameter of the Tube	14.0 mm
Axial Length of the Tube	80 mm
Number of Rings	0, 1 and 2
Actual l_0/d_0 (Ring0: Ring1: Ring2 = [5.71: 2.92: 1.86])	
Load	0.0N, 20N 40N

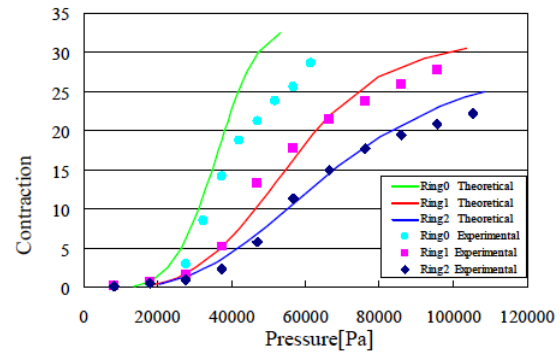


Fig. 7 Comparison between the theoretical and experimental results of the relationship between the pressure and contraction ratios as a function of l_0/d_0 .

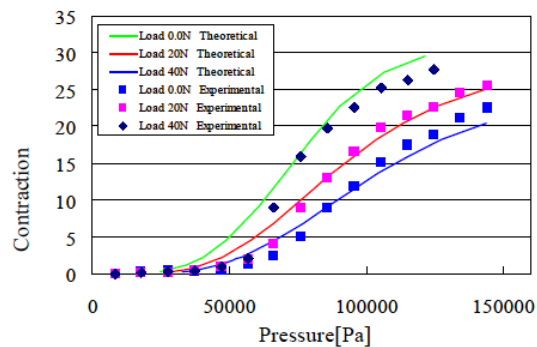


Fig. 8 Comparison between the theoretical and experimental results of the relationship between the pressure and contraction ratio as a function of the loads.

an Electro-Pneumatic Proportional Valve.

The condition of the artificial muscle was measured by a displacement sensor, pressure sensor and load sensor. All of the measured signals were recorded in a PC through an AD converter. Table 1 shows the specifications of the artificial muscle. Actually, the ratio l_0/d_0 corresponded to the number of rings, such that Ring0: Ring1: Ring2 = [5.71: 2.92: 1.86]. The value of the underlined part is the normal specification.

B. A Changing ratio of l_0/d_0

Fig. 7 shows the result of the comparison between the theoretical and experimental results of the relationship between pressure and contraction ratio as a function of l_0/d_0 . At low pressures, both the theoretical and experimental results show that as the ratio l_0/d_0 increases, the contraction ratio increases as well. One characteristic of this artificial muscle is a sudden rise in the contraction ratio in the middle level of pressures; the mathematical and experimental results were similar. The mathematical model adequately corresponded to the change of the ratio l_0/d_0 , but the experimental result of Ring0 was smaller than the theoretical result. This is because rubber is non-linear; hence the geometric model was not a circle.

C. A Changing of load

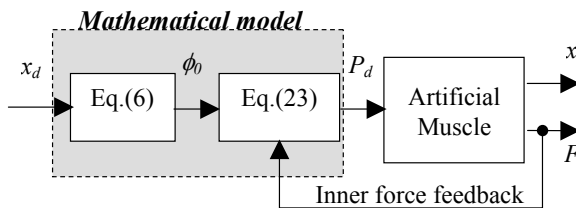


Fig.9 A block-diagram of the position control of the artificial muscle

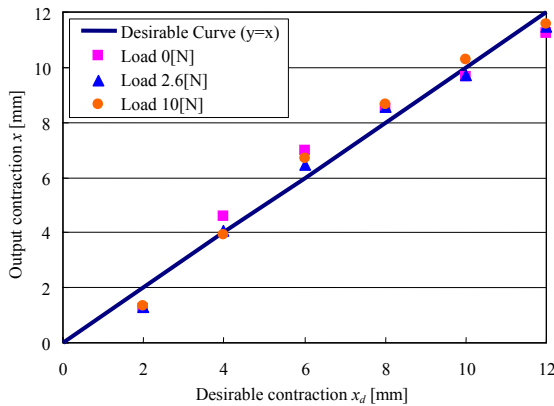


Fig. 10 Comparison between the desired curve and experimental results of the relationship between the inputs and linearized outputs.

Fig. 8 shows the result of comparing the theoretical and experimental results of the relationship between the pressure and contraction ratio as a function of the loads. This comparison shows that the theoretical and experimental results are almost the same, even with a change in the load parameter at the middle of the pressure range.

V. POSITION AND FORCE CONTROL OF THE ARTIFICIAL MUSCLE

A. Composition of Position control based on the mathematical model

If the contraction x has a target value x_d , the pressure P_d given by eq. (23) is the pressure to realize the target value x_d . Therefore, the contraction x to get pressure P and the target value x_d is a linear relationship. In this paper, these previous compensations are called the feed-forward linearization. If this method can be applied to this artificial muscle, the muscle will be easier to use in a mechanical system because the differences in shape parameters such as the l_0/d_0 , the thickness of the tube, etc. can be taken into consideration. Furthermore, by substituting the measured force for F_l in eq. (23) as inner feedback, the influence of the load on the position control can be reduced. Fig. 10 shows the experimental result of the position control using the feed-forward linearization as a parameter of the load. At a low-pressure level, error occurs, but there was no sudden rise at a middle level of pressure. This shows a good linear relationship.

Dynamic characteristics of the position control are important. Fig. 11 shows the dynamic characteristics of the artificial muscle without inner force feedback. In this figure,

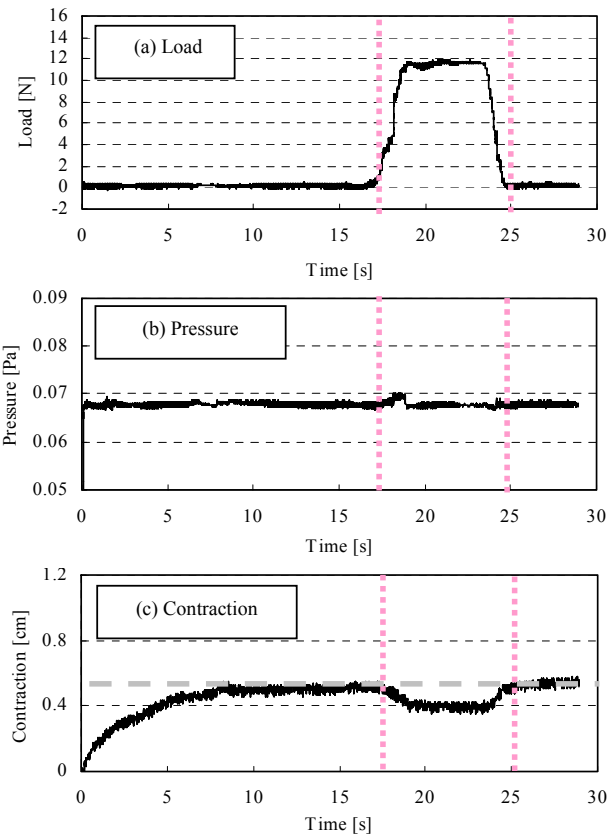


Fig.11 Dynamic characteristics of the artificial muscle without force inner feedback.

we can see that the variation in the contraction distance is caused by changing the load characteristics since the pressure cannot correspond with changes in the load. Therefore, the artificial muscle must be controlled by the pressure that adjusts to an arbitrary load. Fig. 12 shows the dynamic characteristics of the artificial muscle in the case of the application of inner force feedback. The contraction of this artificial muscle can maintain the target value because pressure is controlled to an appropriate value by inner feedback according to changes in the load.

B. Composition of the force control based on the mathematical model

We next discuss the force control of the artificial muscle. A block diagram of the force control of the artificial muscle based on the mathematical model is shown in Fig. 13. This control system is created by substituting the measured contraction distance for x in eq. (6) as an inner feedback. Further, by using F_l in eq. (23) as the target value F_d , the target force can be specified. Fig. 14 shows the experimental results of the relationship between the target forces and measured forces as a parameter of the contraction distance when applying the proposed force control system. As is shown in this figure, the measured force exists near the target value even though the contraction distances have

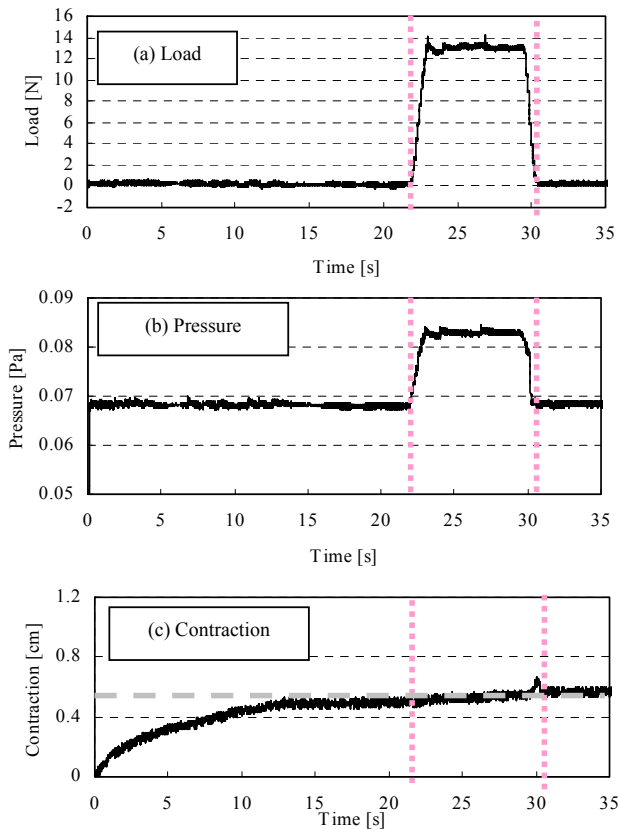


Fig.12 Dynamic characteristics of the artificial muscle with force inner feedback.

changed. Therefore, it confirms that the force of this artificial muscle is controlled by the proposed method.

In the future, by applying an outer force feedback control (the broken line in Fig.13), the measured force will be more precisely controlled. Furthermore, if the position and the force control were to be combined, the determination of the compliance control could be realized.

6. CONCLUSIONS

In this paper the derivation of a mathematical model of the artificial muscle reinforced by straight fibers is realized and examined by feed-forward linearization. Our results show the following:

1. The derived mathematical model and the experimental results adequately corresponded to changes in the ratio l_0/d_0 and the load.
2. The proposed position control based on the mathematical model as a prior compensation was applied to the artificial muscle. The result was targeted, and the output value showed a good linear relationship.
3. The proposed force control was applied to the artificial muscle. As a result, the force of this muscle is controlled to the target value.

In the future, we would like to discuss how this type of artificial muscle can be applied to a soft robot manipulator.

REFERENCES

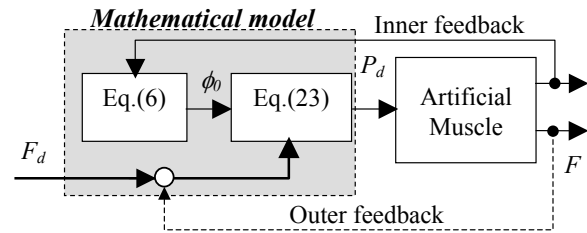


Fig.13 A block diagram of the force control of the artificial muscle

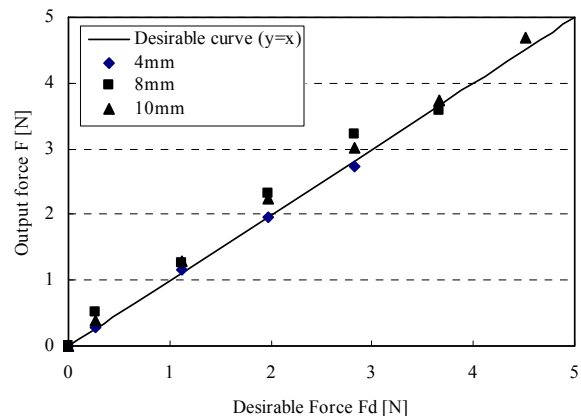


Fig. 14 Comparison of the experimental results of the relationship between the inputs and linearized outputs as a function of the contraction distance.

- [1] Toshiro Noritugu et al., Control Performance of Rubber Artificial Muscle. *Trans. of JSME C*, Vol. 60, No.570, pp.193-198 (1994).
- [2] Hiroshi Kobayashi, New Robot Technology Concept Applicable to Human Physical Support -The Concept and Possibility of the Muscle Suit, *Journal of Robotics and Mechatronics*, Vol.14 No.1, pp.46-53 (2002).
- [3] N. Saga and T. Nakamura et al., Development of artificial muscle actuator Reinforced by Kevlar Fiber. *Proceedings of IEEE ICIT2002*, pp. 950-954 (2002).
- [4] Carlo Ferraresi et al., Flexible Pneumatic Actuators: A comparison between The McKibben and the Straight Fibers Muscle. *Journal of Robotics and Mechatronics*, Vol.13 No.1, pp.56-63 (2001)..
- [5] Taro Nakamura et al., Development of a Pneumatic Artificial Muscle based on Biomechanical Characteristics., *IEEE ICIT2003*, pp.729-734 (2003).
- [6] Nickel, V.L., Perry, and Garrett, A.L. Development of useful function in the severely paralysed hand. *Journal of Bone and Joint Surgery*, 45A(5), pp.933-952 (1963).
- [7] Hill, A. V., The heat of shortening and the dynamic constants of muscle. *Proc. of Royal Society of London*, B.126, pp.136-195 (1938).
- [8] C.P. Chou, B. Hannaford, Static and Dynamic Characteristics of McKibben Pneumatic Artificial Muscles. *Proc. of IEEE ICRA'94*, pp.281-286 (1994).
- [9] Toshiharu Kagawa et al., Power Assist Circuit using Artificial Muscle, *Trans. of JSME C*, Vol. 59, No.564, pp.112-118 (1993).]